Empirical Design Technique for Management and GMPLS-Signaling Communication Networks

Atsushi Taniguchi(1), Yukio Tsukishima(1), Wataru Imajuku(1), Kaori Shimizu(2), Rie Hayashi(2)
Ichiro Inoue(2), Kazuto Noguchi(3) , Masahiko Jinno(1), and Shigeo Urushidani(4)
1 : NTT Network Innovation Laboratories, 1-1 Hikari-no-oka, Yokosuka, Kanagawa 239-0847 Japan,
atsushi.taniguchi@ntt.com
2 : NTT Network Service Systems Laboratories , 3-9-11 Midori-cho, Musashino, Tokyo 180-8585 Japan
3 : NTT Service Integration Laboratories, , 3-9-11 Midori-cho, Musashino, Tokyo 180-8585 Japan
4 : National Institute of Informatics, 2-1-2 Hitotsubashi, Chiyoda, Tokyo 101-8430 Japan

***Abstract*- A technique to design signaling and management communication networks (SCN and MCN) is proposed based on experiments using a GMPLS-enabled network. This design technique will provide SCNs and MCNs with a sufficient bandwidth for packet loss-free and jitter-less transmission.**

Keywords: Optical communication, Communication system signaling, communication system operation and management, distributed control

I. INTRODUCTION

The Generalized Multi-Protocol Label Switching (GMPLS) technology [1,2] is a framework that unifies network control of various types of network elements across multiple network layers. This framework enables network operators to simplify the development of network control functionalities in their network management systems (NMSs). Generally, a NMS issues a path-provisioning order to a GMPLS-enabled node via a management communication network (MCN) [2-4]. Then GMPLS-enabled nodes send and receive extended ReSource reserVation Protocol with Traffic Engineering (RSVP-TE) [5] messages to provide a path over the transport plane via a signaling communication network (SCN) with the help of extended Open Shortest Path First (OSPF) messages [6] to manage the transport plane network.

The SCN and MCN should have sufficient bandwidth to prevent such control and management messages from packet overload. This is because when a link or node failure occurs, recovering the failed link or node via the GMPLS restoration scheme should be completed as soon as possible [7]. If the SCN and the MCN do not have sufficient bandwidth to prevent packet overload, buffering causes an excessive delay and results in slow GMPLS-based restoration. Thus, an appropriate design technique for SCNs and MCNs is required.

Some studies have reported SCN design techniques [8]. However, it is very difficult and unrealistic to design MCNs and SCNs using only network simulators. Although the GMPLS signaling messages in the SCN are standardized by Internet Engineering Task Force (IETF) RFC 3945 [1], path-provisioning messages sent from the NMS in the MCN depend on the implementation of the switch vendors. Unfortunately, no design technique has been proposed based on experimental results on an SCN and an MCN. To design these networks appropriately, it is essential to evaluate the vendor specific and non-standard management messages that are sent over the MCN.

In this paper, we propose an empirical technique to design SCNs and MCNs based on experimental evaluation of those networks. In the proposed process, the measurement data contained in management messages are utilized to estimate the required capacity of links in the MCN. Also the concurrency of the GMPLS signaling messages is analyzed to estimate the overall bandwidth of the SCN and the MCN. Such integrated analysis of the SCN and MCN based on empirical knowledge provides a more realistic design technique for these networks with sufficient bandwidth for packet-loss-free and jitter-less transmission.

II. EMPIRICAL DESIGN TECHNIQUE

A. Architecture of SCN and MCN

SCNs and MCNs are basically established based on the two types of network topologies described below. Figures 1(a) and 1(b) show a real and a virtual partitioning model, respectively. In the real partitioning model, the SCN and the MCN are established independently and have simple configurations. Therefore, a link or node failure can be specified easily when a failure occurs in the SCN or MCN. On the other hand, in the virtual partitioning model, the SCN and the MCN are overlapped over the same network, and are virtually divided using network virtualization technologies such as a Virtual Local Area Network (VLAN), Virtual Private Network (VPN), and Generic Routing Encapsulation (GRE) tunneling. Hence, the virtual partitioning model can reduce the number of network elements required to construct the SCN and the MCN compared to that required for the real partitioning model. These models will be employed properly depending on the Capital Expenditure (CAPEX), Operating Expenditure (OPEX), reliability and so forth. Therefore, a design technique that can be applied to both models is required.

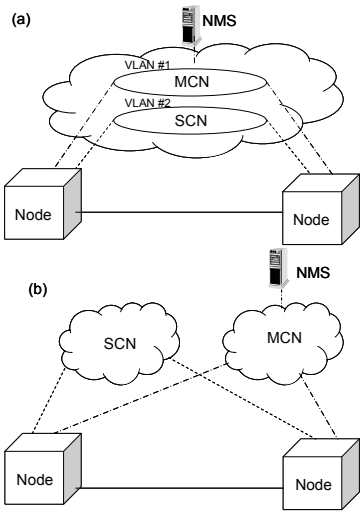

Figure 1. Real and virtual partitioning models.
(a) and (b) show the virtual and real partitioning models, respectively.

B. Proposed technique to design required link capacity in SCNs and MCNs

To estimate the required capacity of links in an SCN and an MCN, a path provisioning sequence should be analyzed. Figure 2 illustrates an example of the messaging sequences among the NMS and GMPLS-enabled ingress, transit, and egress nodes for creating virtually concatenated VC-4 paths. The bandwidth between the ingress and egress nodes is changed per VC-4 path to dynamically and finely adjust it without packet-loss.

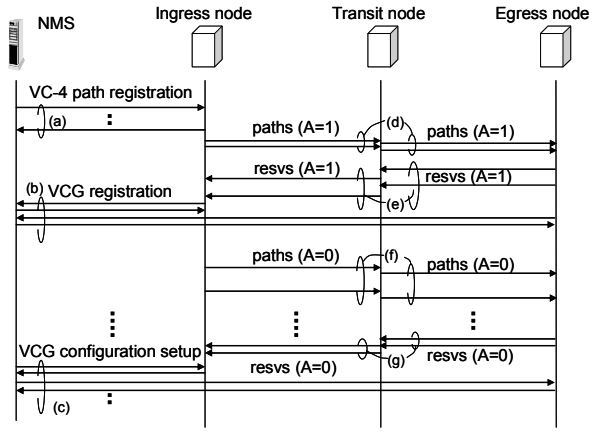

Figure 2. Messaging chart for establishing virtually concatenated VC-4 paths

In the initial state, the NMS negotiates with the ingress node at the termination point of the VC-4 paths in order to establish the VC-4 paths. Then the ingress node and the other nodes on the VC-4 paths exchange GMPLS signaling messages, and establish the VC-4 paths between the ingress and egress nodes. Next, the NMS negotiates with all the nodes along the VC-4 paths to configure the virtual concatenation group (VCG). As defined by IETF RFC 3946 [9], the VC-4 paths are physically configured by a pair comprising path (A=1) and resv (A=1) messages, and VC-4 paths are activated by a pair comprising path (A=0) and resv (A=0) messages. As shown in Fig. 2, multiple VC-4 paths are sequentially established for each VCG in terms of path-data synchronization between the NMS and the nodes. Therefore, the processes for establishing virtually concatenated VC-4 paths do not overlap each other. Moreover, RSVP hello, OSPF hello, and LSU messaging sometimes overlap RSVP signaling messages.

The messaging processes from (a) to (g) shown in Fig. 2 are partially dependent on the NMS and the node implementations, but they are basic and intrinsic processes. Therefore, we propose a design technique for the required link capacity in an SCN and an MCN based on this messaging sequence.

Before discussing the details of the design technique, judging from the current status of commercially available switches, we note that the proposed design technique does not take into consideration a priority control mechanism in the SCN and the MCN. On the other hand, we assume the requirement that GMPLS signaling and management messages are not delayed even in a possible bursty traffic state. This means that experimental evaluation of the peak rate of burst traffic is required before the determination of the link capacity of the SCN and the MCN.

First, we propose the following assumptions which are the essential conditions and the fundamental parameters for the purpose of formulating the required capacity of the links in the SCN and the MCN.

(1) Burst traffic is possibly generated in processes (a)-(g), since occasionally multiple VC-4 paths are concurrently created in GMPLS-enabled networks. The required link capacity in the MCN is the highest among the throughput of (a)-(c). On the other hand, the required link capacity in the SCN is equal to the highest among the throughput of (d)-(g).
(2) Messaging processes from (a) - (g) do not overlap each other in the same direction in the same link within the minimum packet interval time of links in the SCN and the MCN.
(3) Each peak rate of processes (a)-(g) is given by S/T where S is the packet size and T is determined based on the NMS and the node performance, and T is far larger than the minimum packet interval time of links in the SCN and the MCN.

If assumptions (1)-(2) are correct, the required link capacity in a real partitioning-based MCN (*MCN-link*) is given by Eq. (A).

$$MCN\text{-}link = max((a), (b), (c)) \quad \text{(A)}$$

max(X, Y, Z): The highest of the traffic rates of *X, Y,* and *Z*

The required link capacity in a real partitioning-based SCN (*SCN-link*) is given by Eq. (B).

$$SCN\text{-}link = max((d)\text{-}(g)) + OL + OH + RH + LH \quad \text{(B)}$$

max(X-Y); the largest one of the traffic rates from *X* to *Y*
OL: Traffic rate of OSPF LSU between adjacent nodes
OH: Traffic rate of OSPF hello between adjacent nodes
RH: Traffic rate of RSVP hello between adjacent nodes
LH: Traffic rate of LMP hello between adjacent nodes

The required link capacity in a virtual partitioning-based SCN and MCN (*SCN_MCN-link*) is given by Eq. (C).

$$SCN\_MCN\text{-}link = max(SCN\text{-}link, MCN\text{-}link) \quad (C)$$

The packet sizes for path (A=1), resv (A=1), path (A=0), resv (A=0) messages and the Acks for those messages are standardized by the IETF. The size of the packets traversing over the MCN is equal to or less than 1526 bytes which is the maximum transmission unit (MTU) over Ethernet. If assumption (3) is correct, we can estimate the performance of the NMS and that of GMPLS by obtaining *T*, and we can accurately design the SCN-link, the MCN-link, and the SCN_MCN-link.

On the other hand, if *T* is nearly equal to the minimum packet interval time which is equal to the MTU divided by the line rate, the links do not have sufficient bandwidth for packet-loss-free and jitter-less transmission. In other words, *T* depends mainly on the band limitation of the links in the SCN and the MCN. Therefore, we cannot in any way accurately estimate the SCN-link, the MCN-link, and the SCN_MCN-link.

To evaluate the validity of the assumptions and to obtain *T,* which depends on the performance of the NMS and the nodes, we must evaluate the actual behaviour of the network equipment.

C. Topology dependence of link capacity ratio

Figure 3 illustrates the network topologies of the SCN and the MCN using the virtual partitioning model with full-meshed transport networks of six nodes. Figure 4 shows the highest required link capacity of all links to transport GMPLS signaling messages when end-to-end fully meshed paths are provided among all GMPLS-enabled nodes.

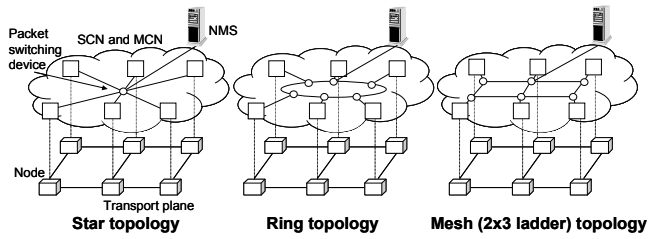

Figure 3. Network topology types for SCN and MCN with meshed transport network of six nodes

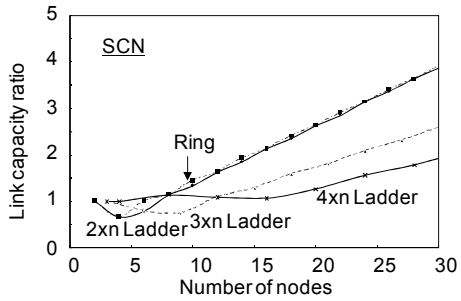

Figure 4. Required link capacity based on network topology types for SCN in comparison to start topology when end-to-end fully meshed paths are coincidentally provided among all nodes.

Based on ITU-T draft G.7712 [4], the SCN and the MCN topologies are illustrated as basic network topology types such as a star, a ring, or a mesh including a ladder. The NMS is located in the same place where one of GMPLS-enabled nodes is established. These topologies will be used properly depending on the CAPEX, the OPEX, reliability and so forth. Basically, the star topology reduces the number of links in a network. On the other hand, a mesh topology provides high reliability to end-to-end paths between GMPLS-enabled nodes. A ring topology reduces the number of links in a network compared to the mesh topology, and provides higher reliability to end-to-end paths between GMPLS-enabled nodes than that provided by the star topology. In Fig. 4, the horizontal axis shows the number of GMPLS-enabled nodes. The vertical axis shows the link capacity ratio of the ring and the mesh topologies to the star topology. When the number of nodes is less than 12, the ring and the mesh topologies are better than the star topology in terms of the required link capacity. On the other hand, when the number of nodes is equal to or larger than 12, the link capacity ratio of the star topology is less than those of the mesh and the ring topologies.

Figure 5 shows an MCN, a transport network and the location of the NMS. Figure 6 shows the required link capacity ratio of the links of the networks illustrated in Fig. 5 that transport messages between the NMS and GMPLS-enabled nodes when end-to-end full meshed paths are coincidentally provided. The vertical axis indicates the link capacity ratio of the ring and the mesh topologies to the star topology. Basically, the traffic between the NMS and GMPLS-enabled nodes is evenly load-balanced over the links connected to the NMS. Therefore, the link capacity depends on the number of those links. As shown in Fig. 6, the required link capacity ratio of the ring topology is expected to decrease to approximately 50 %, and the required link capacity of the mesh network shown in Fig. 4(c) is expected to decrease to approximately 30 %.

As a result, by estimating the required link capacities of the SCN and MCN topologies, we can also estimate the required link capacity against the other SCN and MCN topologies.

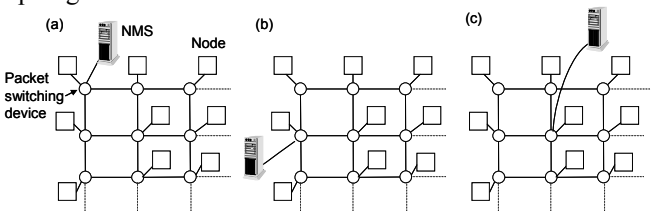

Figure 5. Location of NMS with full-meshed SCN and MCN

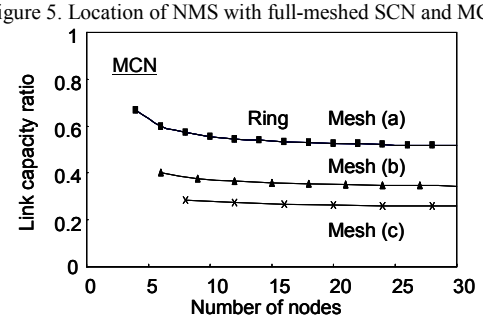

Figure 6. Required link capacity based on network topology types for MCN in comparison to star topology when end-to-end fully meshed paths are coincidentally provided among all nodes.

III. EXPERIMENTAL NETWORK CONFIGURATION AND RESULTS

A. Experimental configuration

To ensure the design technique proposed in Section II, we verify the validity of the assumptions and evaluate the required link capacity by analyzing the experimental results. Figure 7 illustrates the experimental configuration. This network consists of six next-generation SONET/SDH nodes (L1SWs) with GMPLS, GFP, VCAT, LCAS, and virtual container-4 (VC-4) switching capabilities.

For the transport plane network, the L1SWs are located at the NII site [10] and NTT Musashino R&D site, and are connected by STM-64 links via GEMnet 2 [11]. The SCN and MCN are overlapped on the same network, which comprises Ethernet switches (L2SWs) and 100 Mbit/s Ethernet links. In addition, the SCN and MCN are virtually divided using two of the tagged VLANs.

By using this experimental network environment, we evaluate the validity of the assumptions and the equations in Section II.

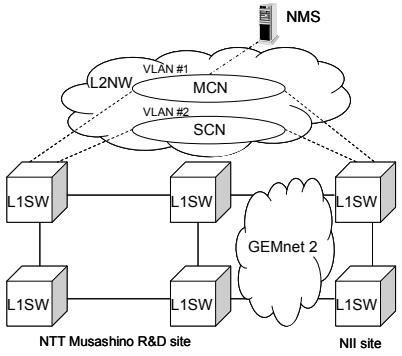

Figure 7. Experimental configuration

B. Evaluation of OSPF and RSVP traffic rates

First, the total traffic rate of the OSPF LSU is measured. When VC-4 paths are established via GMPLS signaling, the OSPF LSU simultaneously traverses over the SCN, and its traffic rate is equal to or less than 1 Mbit/s.

Next, the traffic rates of OSPF and RSVP hello messages are measured. The interval for each OSPF and RSVP hello message is configured to be 10 seconds in this experiment. The traffic flows are nearly equal to or less than 100 bit/s.

In other words, *OL*, *OH*, and *RH* represent 1 Mbit/s, 100 bit/s, and 100 bit/s, respectively.

C. Validation of assumption (1)

Figures 8(a) and 8(b) illustrate a sample of the monitored traffic patterns in the SCN and MCN when the 64 VC-4 paths (VC-4-64v) are established via GMPLS, respectively. They show the traffic rates as a function of the elapsed time on the microsecond time scale. Figure 8(a) shows the traffic streaming from the ingress node to the egress node, and Fig. 8(b) shows the traffic traversing from the ingress node to the NMS.

In the SCN, the first burst traffic flow is generated by path (A=1) messaging, and it is the highest traffic rate. This is the reason why path (A=1) messages are sent together. On the other hand, path (A=0) and the Ack messages for GMPLS signaling also generate a second burst traffic flow. However, these messages are transmitted sporadically using the sequential confirmation and configuration processes for L1 cross connections against those messages, and thus the traffic rate is lower than that for path (A=1). Next, the traffic comprising the resv messages from the egress node to the ingress node forms a very similar pattern as that illustrated in Fig. 8(a), but it is smaller. Therefore, the traffic from the egress node to the ingress node is negligible in terms of designing the required capacity for the links in the SCN.

On the other hand, in the MCN, only burst traffic is generated by VCG configuration messages. The other messages in the MCN are sent sporadically for the same reason that the path (A=0) messages are sent sporadically. Therefore, the traffic rates for these messages are far lower than that of the above peak traffic, and are negligible in terms of designing the required capacity for the links in the MCN. Figure 8(b) shows that the peak traffic rate of the VCG configuration messages is the highest traffic rate because the VCG configuration information with a large data size is fragmented and mapped into multiple messages based on the MTU, and those messages are transmitted together. Next, the traffic from the NMS to the egress node, the traffic from the NMS to the ingress node, and the traffic from the egress node to the NMS form very similar patterns as illustrated in Fig. 8(b). However, these traffic rates are far lower than that from the ingress node to the NMS. Therefore, they are negligible in terms of designing the required capacity for the links in the MCN.

As a result, the required capacity of the links in the SCN is confirmed to be the traffic rate of the path (A=1) messaging, and the required capacity of links in the MCN is also confirmed to be the traffic rate of the VCG configuration setup messaging.

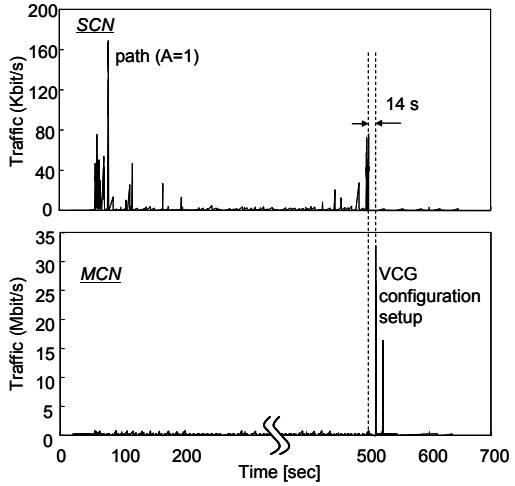

Figure 8. Sample of the monitored traffic patterns in provisioning VC-4-64v paths. (a) and (b) show control traffic from the ingress node to egress node and the traffic from ingress node to NMS, respectively

D. Validation of assumption (2)

In these experiments, the burst traffic in the SCN and the MCN is generated across an average interval of greater than 0.1 second per VC-4 path, that is, the path (A=1) messaging does not overlap the other burst traffic in the SCN and the MCN. For example, the path (A=1) messaging does not overlap the VCG configuration setup messaging.

In other words, the messaging processes from (a) to (g), which are shown in Fig. 2, do not overlap each other in

the same direction in the same link in the SCN and the MCN.

E. Validation of assumption (3)

Figures 9(a) and 9(b) show the measured traffic rate from the ingress node to the egress node over the SCN and the MCN, the packet interval time (dotted line), and the calculated traffic peak rate using the packet interval time (dash-dotted line), respectively. As for the calculated traffic peak rate, *S* of path (A=1) is 314 [bytes], which is standardized by [5]. On the other hand, *S* of the MCN is 1526 [bytes], which is the MTU of the links in the SCN and the MCN. We confirm that the packet interval time is determined by the performance of the NMS and the L1SW because that the packet interval time is greater than the minimum packet interval of the links (= 1526 [byte]/100 [Mbit/s]) in the SCN and MCN.

As shown in Figs. 9(a) and 9(b), the calculated peak rate is close to the measured peak rate for creating the VC-4-64v paths. Thus the peak traffic rates determine the required capacity of the links in the SCN and the MCN using the measured packet interval times and the measured packet sizes.

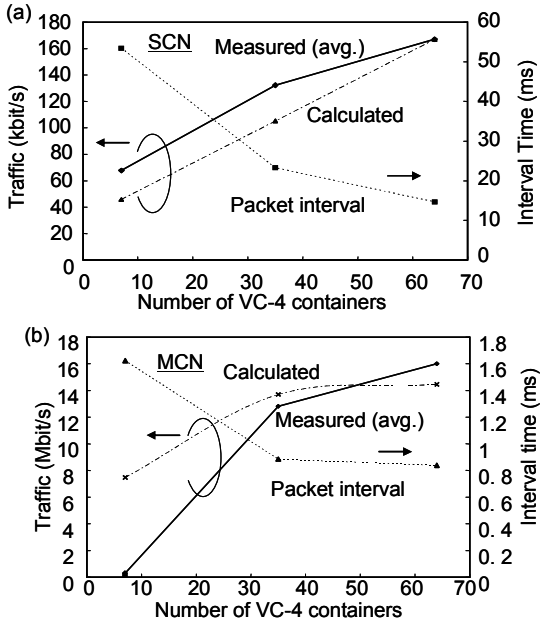

Figure 9. Measured peak traffic rate (solid line), packet interval time (dotted line) and calculated peak traffic rate (dash-dotted line) over (a) SCN and (b) MCN when the LSP is established.

F. Results of validation and discussion

In the above experiments, the validity of assumptions (1)-(3) and Eqs. (A)-(C) in Section II is successfully demonstrated. Table I gives the measured values for the packet interval and the packet size in the experiments, and presents the appropriate SCN-link and MCN-link given by the experiments. This table gives the average of five samples regarding *T* for the SCN-link, *T* for the MCN-link, the SCN-link, and the MCN-link.

The following equations are formulated based on Eqs. (A)-(C), assumptions (1)-(3), and Table I.

In the real partitioning model:

$$MCN\text{-}link\ [\text{bit/s}] = 1526 \times 8 / T \quad (1)$$

$$SCN\text{-}link\ [\text{bit/s}] = 314 \times 8 / T + 1000 + 100 + 100 \quad (2)$$

In the virtual partitioning model:

$$SCN\_MCN\text{-}link = MCN\text{-}link = 1526 \times 8 / T \quad (3)$$

TABLE I
Packet Interval Time for SCN and MCN. SCN-link and MCN-link are not dependent on the number of virtually concatenated VC-4 paths.

Provisioned VC-4 paths	*T* for SCN-link	SCN-link	T for MCN-link	MCN-link
VC-4-7v	53 ms	46 kbit/s	1.6 ms	8 Mbit/s
VC-4-35v	23 ms	105 kbit/s	0.9 ms	14 Mbit/s
VC-4-64v	15 ms	167 kbit/s	0.8 ms	15 Mbit/s

As illustrated in Table I, when SCN and MCN are established over a data communication network, the link capacity of the data communication network would be more than 15 Mbps (in VC-4-64v provisioning). Moreover, the upgrading of the NMS and the L1SWs (e.g. CPU, Memory, HDD…) will cause a shortening of T, and as a result, a larger SCN-link and a larger MCN-link will be required.

IV. CONCLUSION

We proposed a design technique for the SCN and the MCN in GMPLS-enabled network with a sufficient bandwidth to avoid packet overloads based on empirical knowledge. We anticipate that the proposed design technique will be applied to a GMPLS-enabled network to achieve a higher level of reliability in the SCN and the MCN.

REFERENCES

[1] E. Mannie (Editor), "Generalized Multi-Protocol Label Switching (GMPLS) Architecture," IETF RFC3945, 2004.
[2] S. Urishidani et al., "Implementation of Multilayer VPN Capabilities in SINET3," ECOC 2007.
[3] T. Takeda et al., "Layer 1 virtual private networks: Service concepts, architecture requirements, and related advances in standardization," IEEE Commun, Mag., vol. 42, no. 6 pp. 132-138, June 2004.
[4] ITU Recommendation G.7712/Y.1703, "Architecture and specification of data communication network," (ITU 2003).
[5] L. Berger, (Editor), "Generalized Multi-Protocol Label Switching (GMPLS) Signaling Resource ReserVation Protocol-Traffic Engineering (RSVP-TE) Extensions," IETF RFC3473, Jan. 2003.
[6] K. Kompella (Editor), "OSPF Extensions in Support of Generalized Multi-Protocol Label Switching," IETF RFC4203, October 2005.
[7] W. Imajuku et al., "GMPLS Based Survivable Photonic Architecture," IEICE Trans. Commun., vol. E90B, no. 8, pp. 1952-1959.
[8] G. Li et al., "Control plane design for reliable optical networks," IEEE communication magazine, vol. 40, no. 2, Feb., 2002, pp. 90-96.
[9] E. Mannie (Editor), "Generalized Multi-Protocol Label Switching (GMPLS) Extensions for Synchronous Optical Network (SONET) and Synchronous Digital Hierarchy (SDH) Control," IETF RFC3946, 2004.
[10] http://www.nii.ac.jp/
[11] H. Uose, "GEMnet2: NTT's New Network Testbed for Global R&D," in Proceedings of International conference on Testbeds and Research Infrastructures for the Development of Networks and Communities (TRIDENTCOM), 2005, pp. 232-241.